Structural Model Verification with Linear Quadratic Optimization Theory

Helene Lapierre* and Germain Ostiguy†
Ecole Polytechnique, Université de Montreal, Montreal, Quebec, Canada

A graphic tool is developed and validated for the verification and updating of large structure finite element models (FEM) for better correlation with modal test data. The elaborated Linear Quadratic Optimization (LQO) theory consists of a linearization and solution of the conventional matrix optimization problem that respect the connectivity of the structure and the symmetry of the stiffness matrix. The LQO theory is validated through a numerical and experimental sensitivity analysis. The results demonstrate the ability of the LQO algorithm to identify and update the stiffness coefficients associated with the inappropriately modeled load paths in the structure.

Nomenclature

A = constraint matrix (r,p) to be identified by the LQO software
B = constraint matrix $(r,1)$ to be identified by the LQO software
C = transformation vector $(p,1)$ to be identified by the LQO software model
CF_{ij} = confidence factor associated with $K_{A,ij}$
K = updated stiffness matrix (n,n) for the finite element model
K_A = initial analytical stiffness matrix (n,n) of the finite element model
K_A^* = exact analytical stiffness matrix (n,n)
L = Lagrange function
M = mass matrix (n,n)
M_A = analytical mass matrix (n,n)
M_A^* = exact analytical mass matrix (n,n)
m = number of measured modes
n = number of degrees of freedom
p = number of optimization parameters
Q = transformation matrix (p,p) to be identified by the LQO software
r = number of dependent constraints
X = optimization parameter vector $(p,1)$ of the reordered nonzero terms of the upper triangle of the stiffness matrix
$\{\Delta f\}$ = difference between the measured results and the predictions from the finite element model
ΔK_A = corruption of stiffness matrix K; $K_A + \Delta K_A \simeq K_A^*$ (n,n)
$\{\Delta x\}$ = difference between the researched finite element parameters and their initial values
$[\delta f/\delta x]$ = Jacobian matrix
λ = Lagrange multiplier vector $(r,1)$
λ_A^* = exact analytical eigenvalues $(n,1)$ or $(m,1)$
λ_E = measured eigenvalues $(m,1)$
Φ_A = analytical eigenvectors (n,n) or (n,m)
Φ_A^* = exact analytical eigenvectors (n,n) or (n,m)
Φ_E = measured eigenvectors (n,m)
Ω_E^2 = diagonal matrix of measured eigenvalues (m, m)

Presented as Paper 88-2360 at the AIAA/ASME/AHS/ASCE 29th Structures, Structural Dynamics and Materials Conference, Williamsburg, VA, April 18-20, 1988; received July 18, 1988; revision received June 12, 1989.

*Research Assistant; currently Mechanical System Engineer, SPAR Aerospace Limited, Ste-Anne-de-Bellevue, Quebec, Canada.
†Professor, Department of Mechanical Engineering.

Introduction

WHEN the modal predictions of numerical analyses differ from the modal results measured from prototypes, a correlation process must be initiated to adjust the model of the structure analyzed. The elaborated Linear Quadratic Optimization (LQO) theory consists of a linearization and solution of the conventional matrix optimization problem to insure that, first, the initial connectivity specification of the structure analyzed is preserved during the updating process, and, second, that the eigensolution associated with the mass and updated stiffness matrices leads to the measured eigenvalues and eigenvectors.

The problems associated with model verification are numerous: the manipulation of large matrices, the use of incomplete models, and the connectivity preservation issue are some of them. Fundamentally, the objective of every correlation algorithm is to identify the changes in the analytical stiffness and/or mass matrices of the finite element model for which the eigensolution of the updated matrices will lead to the measured frequencies and mode shapes.

$$\{[K_A] - \lambda_E[M_A]\}\Phi_E = 0 \tag{1}$$

Since the early 1970s, several correlation techniques have been developed. The matrix perturbation algorithm developed by Chen and Wada[7] consists of identifying the Jacobian matrix of the system.

$$\{\Delta f\} = \left[\frac{\delta f}{\delta x}\right]\{\Delta x\} \tag{2}$$

The inversion of the Jacobian matrix leads to the updated parameters. This, however, requires a high computational effort for large-scale problems.

Direct model identification procedures have been elaborated to synthesize, directly from the measured eigenvalues and eigenvectors, the mass and stiffness matrices of the structure. The problems encountered by these techniques are of two types. The first is because the order of the system matrices to be synthesized can only equal the number of measured degrees of freedom, which order is, in general, much smaller than the order necessary to describe a complex structure in the full

frequency range for all possible excitation configurations. The second problem is related to the fact that the measured information may be incomplete in the sense that not every mode has been excited during the test. Researchers such as Berman and Nagy,[3] Berman and Wei,[4] and Link[10] have contributed to this area.

The Lagrange multiplier optimization algorithms formulate the correlation problem under a constrained optimization format, the objective being the minimization of the changes in the stiffness and/or mass matrices, and the constraints being the preservation of the orthogonality of Φ_E with respect to M_A^* and the symmetry of K_A. Baruch and Itzhack,[1] and Baruch[2] initiated this approach and Caesar and co-workers[5,6] also contributed, adding additional constraints regarding the consistency of the total mass of the system. Those techniques appear to be extremely well suited to large-scale problems. Their major difficulty, however, is the loss of physical meaning in the updated matrices.

More recently, Kabe[8,9] developed the KMA stiffness matrix updating scheme that tends to preserve a physical meaning in the updated stiffness matrix. He formulated three additional requirements:

1) The connectivity between the nodes of the finite element model must be preserved, or the stiffness matrix zero off-diagonal terms must remain null during the updating process.

2) It is inappropriate to weight the stiffness coefficient changes by a function involving the mass matrix because, for a complex spacecraft structure nonstructural items, such as electronic boxes, batteries, and propellant, generally account for over 80% of the total mass.

3) The objective function to be minimized should be such that the stiffness coefficients with numerically small values do not change with substantially greater percentage changes.

The developed KMA procedure involves a significant level of computational effort for large-scale problems.

The LQO theory is a derivative and an application of the Lagrange multiplier optimization theory to a quadratic objective function with linear constraints. Throughout an original and innovative transposition of the conventional optimization problem, a solution is found and formulated algebraically. This readily usable formula for the updated stiffness matrix avoids the use of iterative processes sensitive to computational and convergence problems.

Theory

In order to develop a scheme that respects the connectivity of the structure and the symmetry of the stiffness matrix, the LQO algorithm uses only the nonzero terms of the upper triangle of K_A as optimization parameters, and reorders them in a linear vector.

The basic development of the LQO theory consists of transforming the classical Lagrange multiplier optimization problem known as:

$$\min \epsilon = \tfrac{1}{2}(K - K_A)^T (K - K_A); \text{ objective} \tag{3}$$

$$\text{const} \begin{cases} K\Phi_E - M\Phi_E\Omega_E^2 = 0; \text{ eigensolution} & (4) \\ K - K^T = 0; \text{ symmetry} & (5) \end{cases}$$

into a linear quadratic formulation recognized as

$$\min \epsilon = \tfrac{1}{2}X^TQX + C^TX; \text{ quadratic function} \tag{6}$$

$$\text{const } AX = B; \text{ linear constraints} \tag{7}$$

for which it can be demonstrated that the optimized parameters are given by

$$X = -Q^{-1}C + Q^{-1}A^T(AQ^{-1}A^T)^{-1}(B + AQ^{-1}C) \tag{8}$$

This is shown by choosing the following Lagrange function associated with the optimization problem:

$$L = \tfrac{1}{2}X^TQX + C^TX + \lambda^T(AX - B) \tag{9}$$

where λ is the vector of Lagrange multipliers. Since the solution of the optimization problem annuls the first derivative of the Lagrange function with respect to X, then

$$\frac{\delta L}{\delta X} = X^TQ + C^T + \lambda^TA \tag{10}$$

But since Q is symmetric, it can be shown that

$$A\lambda^T = -QX - C \tag{11}$$

By premultiplying Eq. (11) by Q^{-1}, and using $AX = B$, we have

$$\lambda = -(AQ^{-1}A^T)^{-1}(B + AQ^{-1}C) \tag{12}$$

which applies only if $(AQ^{-1}A^T)$ is of full rank. Since Q is diagonal, this will be true if the rectangular constraint matrix A is of full rank. Once the matrix A is desingularized, Eq. (12) can be substituted into Eq. (11) to give the expression of the optimized solution of Eq. (8).

The constraint matrix $[A]$ and the constraint vector $\{\boldsymbol{B}\}$ are built by converting the product

$$[K][\Phi] \text{ into } [A]\{X\}$$

and the product

$$[M][\Phi][\Omega^2] \text{ into } \{\boldsymbol{B}\}$$

The desingularization of the constraint matrix A is realized by using a singular value decomposition alorithm. By inspecting the singular values of the matrix A, one can find the rank of that matrix and reduce it to a matrix of full rank. Changes must also be made to the vector $\boldsymbol{B}$ once the matrix A has been reduced to full rank, such that the constraint system $AX = \boldsymbol{B}$ still holds.

The transformation of the conventional objective function

$$\text{MIN: } \epsilon = \frac{1}{2}\sum_{i=1}^{n}\sum_{j=1}^{n} CF_{ij}(K_{ij} - K_{A,ij}) \tag{13}$$

into the equivalent form

$$\text{MIN: } \epsilon = \tfrac{1}{2}X^TQX + C^TX \tag{14}$$

reveals that the matrix $[Q]$ is the diagonal matrix of the confidence factors $[CF_{ij}]$ associated with the respective nonzero terms of the upper triangle of the $[K]$ matrix, and that the vector $\{\boldsymbol{C}\}$ is the element-by-element multiplication of the initial vector $\{-\boldsymbol{X}\}$ by the corresponding confidence factors CF_{ij}. By decreasing or increasing the value of the confidence factors, one can impose that a specific area of a structure be more or less easily changed than another. If the user has no knowledge of such areas, a good practice is to set the confidence factors to $CF_{ij} = (1/K_{ij})^3$, such that the small terms of the stiffness matrix are less easily changed then the large ones.

Compatibility Requirements

As can be appreciated from Eq. (4), the order of the stiffness and mass matrices updated by the LQO algorithm must equal the number of measured degrees of freedom in Φ_E. This is achieved by performing a Guyan reduction on the full matrices.[11] The user must be aware that the accuracy of the results obtained with a Guyan reduction is highly dependent on the selection of the analytical degrees of freedom. There are several criteria that must be respected during the choice of the analytical degrees of freedom, but, on the other hand, it ap-

pears that those same criteria also lead to a judicious selection for the location of the accelerometers. Before a test is conducted, the user should insure that the accelerometers are located such that the corresponding Guyan reduction will yield good results. This can easily be done by comparing the Guyan results with the ones obtained from a generalized dynamic reduction.

Numerical Validation

In order to validate the LQO algorithm, an eight-degree-of-freedom numerical structure (Fig. 1) has been used for which the mass and stiffness matrices could be obtained directly by comparing the expressions for the kinetic and potential energy with the quadratic forms. The measured data for this numerical structure have been simulated directly from the analytical eigenvalues and eigenvectors. By imposing a specific corruption inside the initial value of the stiffness matrix, one can then check how accurately the LQO software operates by comparing the computed ΔK_A matrix with the initial corruption. Figure 2 illustrates this scheme.

Three different scenarios are used for the corruption of the initial stiffness matrix. The first scenario consists of using a ΔK_A equal to zero, or no corruption at all. The second consists in using a high level of corruption, this level reaching 100% for some of the coefficients of K_A. For these two first scenarios, the simulated measured frequencies and mode shapes correspond to the exact analytical frequencies and mode shapes.

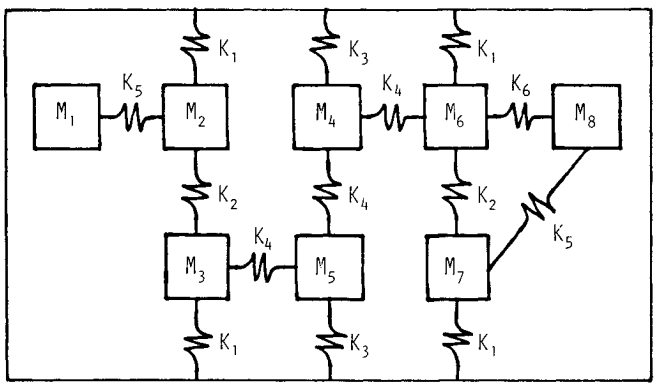

$K_1 = 1000$ $K_2 = 10$ $K_3 = 900$
$K_4 = 100$ $K_5 = 1,5$ $K_6 = 2,0$
$M_1 = 0,001$ $M_8 = 0,002$
$M_j = 1,0$ $j = 2,7$

Fig. 1 Eight-degree-of-freedom numerical system.

The last scenario was built so as to take into consideration the fact that the residues, and thus the shape coefficients, are not only difficult to obtain experimentally, but are extracted from a structure that possesses intrinsic structural damping. In order to recreate those effects on the simulated measured data, a damping ratio of 0.01 was assigned to each analytical mode. The initial corruption of the stiffness matrix for that third scenario is the same as for the second one. This last scenario provides information about the sensitivity of the LQO algorithm to the quality of the measured data.

For the eight-degree-of-freedom numerical system presented in Fig. 1, it appears that the 16 nonzero coefficients in the upper triangle of K_A could be identified by using two normal modes (16/8 = 2). However, by observing degree of freedom no. 6, one can determine that a load path indeterminancy of three is involved. Thus, to obtain an accurate identification of all stiffness coefficients, at least three measured modes – or, more precisely, simulated modes in this case – will be needed.

Results with No K_A Corruption

The results obtained when submitting the LQO algorithm with K_A^* and M_A^* as analytical stiffness and mass matrices, and λ_A^* and Φ_A^* as simulated measured eigenvalues and eigenvectors, are presented in Table 1 and in Fig. 3. One can see from Table 1 that when three measured modes are used, the accuracy of the LQO predicted results is very good. When using less than three measured modes, a loss of accuracy is observed.

Knowing that

$$\left[K_A^* - \lambda_A^* M_A^*\right] \Phi_A^* = 0$$

the LQO tool will be validated if:

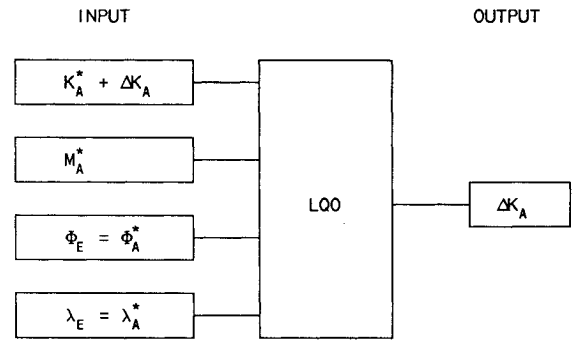

Fig. 2 LQO numerical validation scheme.

Table 1 LQO results with no K_A corruption

Coefficient	Corrupted stiffness coefficient	Exact stiffness coefficient	LQO results 1 mode	2 modes	3 modes	4 modes	5 modes
1.1	1.5	1.5	1.1	1.6	1.6	1.5	1.5
1.2	− 1.5	− 1.5	− 0.4	− 1.8	− 1.7	− 1.4	− 1.5
2.2	1011.5	1011.5	941.5	1012.3	1012.2	1011.2	1011.5
2.3	− 10.0	− 10.0	0.0	− 10.0	− 10.0	− 10.0	− 10.0
3.3	1110.0	1110.0	957.3	1110.2	1110.2	1110.0	1110.0
3.5	− 100.0	− 100.0	− 10.1	− 100.1	− 100.1	− 100.0	− 100.0
4.4	1100.0	1100.0	971.7	1099.9	1099.9	1100.0	1100.0
4.5	− 100.0	− 100.0	− 25.3	− 99.9	− 99.9	− 100.0	− 100.0
4.6	− 100.0	− 100.0	− 10.1	− 100.0	− 100.0	− 100.0	− 100.0
5.5	1100.0	1100.0	972.0	1110.0	1100.0	1100.0	1100.0
6.6	1112.0	1112.0	960.0	1110.0	1111.8	1111.9	1111.9
6.7	− 10.0	− 10.0	− 0.01	− 11.7	− 10.1	− 10.1	− 10.0
6.8	− 2.0	− 2.0	− 0.5	− 0.4	− 1.9	− 1.9	− 2.0
7.7	1011.5	1011.5	940.0	1010.1	1011.4	1011.4	1011.5
7.8	− 1.5	− 1.5	− 0.01	− 0.1	− 1.4	− 1.4	− 1.5
8.8	3.5	3.5	2.2	2.2	3.4	3.4	3.5

Table 2 LQO results with K_A corruption

Coefficient	Corrupted stiffness coefficient	Exact stiffness coefficient	LQO results				
			1 mode	2 modes	3 modes	4 modes	5 modes
1.1	2.0	1.5	1.1	1.6	1.6	1.5	1.5
1.2	−2.0	−1.5	−0.4	−1.8	−1.7	−1.4	−1.5
2.2	1512.0	1011.5	941.5	1012.3	1012.2	1011.2	1011.5
2.3	−10.0	−10.0	0.0	−10.0	−10.0	−10.0	−10.0
3.3	1710.0	1110.0	957.3	1110.2	1110.2	1110.0	1110.0
3.5	−200.0	−100.0	−10.1	−100.1	−100.1	−100.0	−100.0
4.4	850.0	1100.0	971.7	1099.9	1099.9	1100.0	1100.0
4.5	−200.0	−100.0	−25.3	−99.9	−99.9	−100.0	−100.0
4.6	−200.0	−100.0	−10.1	−100.0	−100.0	−100.0	−100.0
5.5	850.0	1100.0	972.0	1110.0	1100.0	1100.0	1100.0
6.6	1714.0	1112.0	960.0	1110.0	1111.8	1111.9	1111.9
6.7	−10.0	−10.0	−0.01	−11.7	−10.1	−10.1	−10.0
6.8	−4.0	−2.0	−0.5	−0.4	−1.9	−1.9	−2.0
7.7	1512.0	1011.5	940.0	1010.1	1011.4	1011.4	1011.5
7.8	−2.0	−1.5	−0.01	−0.1	−1.4	−1.4	−1.5
8.8	6.0	3.5	2.2	2.2	3.4	3.4	3.5

Table 3 Initial cross-orthogonality table ($\Phi_E^T M_A^* \Phi_{A_0}$)

1.00	0.00	0.06	0.07
−0.23	1.00	0.92	−0.35
−0.25	−0.24	1.00	0.92
−0.01	4.36	−0.76	1.00

Table 4 Updated cross-orthogonality table ($\Phi_E^T M_A^* \Phi_{A_f}$)

1.00	0.00	0.00	0.00
0.00	1.00	0.00	0.00
0.00	0.00	1.00	0.00
0.00	0.00	0.00	1.00

Table 5 Uncorrupted and corrupted test modes

	Uncorrupted test mode	Corrupted test mode
Φ_1	0.144	0.130
	0.053	0.048
	0.360	0.356
	0.606	0.610
	0.604	0.601
	0.362	0.365
	0.062	0.068
	0.505	0.522
Φ_2	2.774	2.773
	0.915	0.917
	0.128	0.138
	−0.089	−0.078
	0.042	0.050
	−0.125	−0.123
	−0.336	−0.330
	0.505	−0.498

Results with K_A Corruption

The results obtained with submitting the LQO algorithm with $K_A^* + \Delta K_A$ and M_A^* as analytical stiffness and mass matrices, and λ_A^* and Φ_A^* as simulated measured eigenvalues and eigenvectors, are presented in Table 2. Figure 4 graphically displays the LQO computed ΔK_A matrix. From this output, the user can identify the regions causing the discrepancy between the original predictions from the finite-element model and measured results.

During the execution of the LQO, the initial cross-orthogonality between the measured and analytical modes, with respect to M_A, changed from values shown in Table 3 to the values given in Table 4 after one iteration.

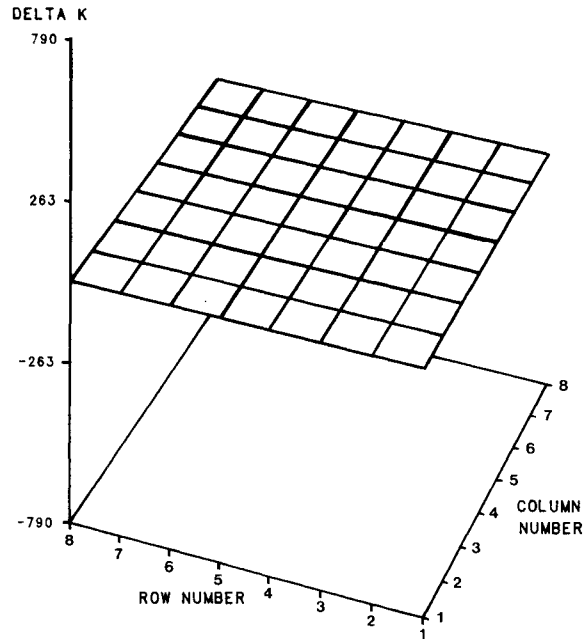

Fig. 3 Graphical presentation of LQO results with no K_A corruption.

Results with Test Modes Corruption

The corrupted test modes were synthesized so as to take into consideration the facts that 1) the physical structure has intrinsic structural damping, and 2) the residues and, thus, mode shape coefficients are difficult to extract.

The discrepancies between the exact analytical mode shapes, Φ_1^*, Φ_2^*, and the corrupted test simulated mode shapes, Φ_1, Φ_2, are shown in Table 5. The corrupted test modes were obtained by computing the forced response of the structure with 1% damping when excited by multiple sinusoidal forces at its first two natural frequencies simultaneously (since only the two first modes were corrupted). A maximum contamination of 10% was tolerated.

The results obtained when submitting the LQO algorithm with $K_A^* + \Delta K_A$, M_A^*, as analytical stiffness and mass matrices and λ_A^*, corrupted Φ_A^*, as simulated measured eigenvalues and eigenvectors are presented in Table 6. The graphical display of those results can be visualized in Fig. 5.

When using corrupted modes, the updated K_A matrix is not strictly positive anymore. This is induced by the existence of negative terms on the diagonal of the updated K_A matrix and it leads to fictitious negative eigenvalues. However, by com-

paring Fig. 5 with Fig. 4, it can be appreciated that even if those anomalies do exist, the results are still meaningful, not so much in an absolute as in a relative sense. Those anomalies are more likely to occur for small stiffness coefficients. This is one reason why we say that the LQO algorithm is a tool and does not replace engineering judgment.

Experimental Validation

The experimental validation of the LQO tool was undertaken to demonstrate the robustness of the LQO algorithm with more realistic structures for which intrinsic experimental inaccuracies exist because of 1) high modal density, 2) difficulty in experimentally extracting residues in relation to different curve fitting techniques, 3) uncertainty in physical boundary conditions during the tests, and 4) structural damping of the system tested.

An experimental structure called TSHAPE (Fig. 6) was designed, analyzed, and tested at the Communication Research Centre of Canada. The TSHAPE structure was tested in a fixed-free configuration and excited with two portable shakers. A total of 63 accelerometers were used to measure the response of the structure. The analysis of TSHAPE was performed by using the MSC/NASTRAN code. A comparison between the numerical predictions and the measured results is made in Table 7.

The TSHAPE numerical data and measured results were submitted to the LQO algorithm for the identification of the inappropriately modeled areas of the structure. The results are presented graphically in Figs. 7 and 8. The inappropriately modeled regions of the TSHAPE structure can be categorized in four distinct groups that correspond to 1) the unmodeled stiffening due to the welds between the horizontal and vertical plates, 2) the interference of the structure with the shaker rod during the test, 3) the unmodeled stiffening because of the bolted masses on the vertical plate, and 4) an inoperative accelerometer.

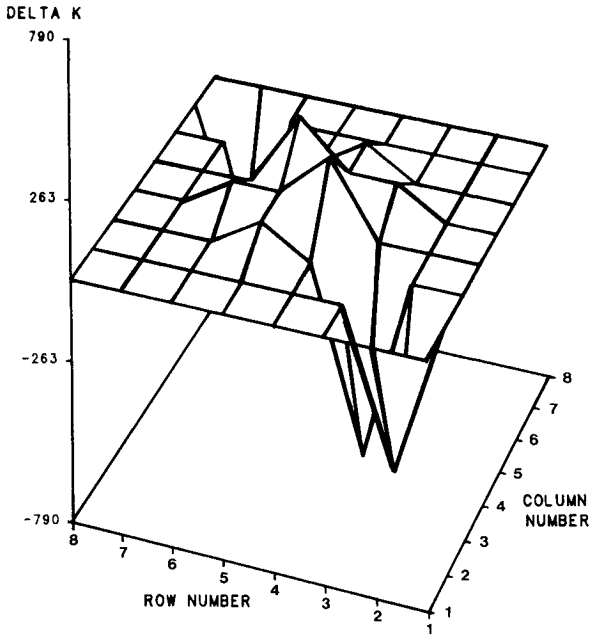

Fig. 4 Graphical presentation of LQO results with K_A corruption.

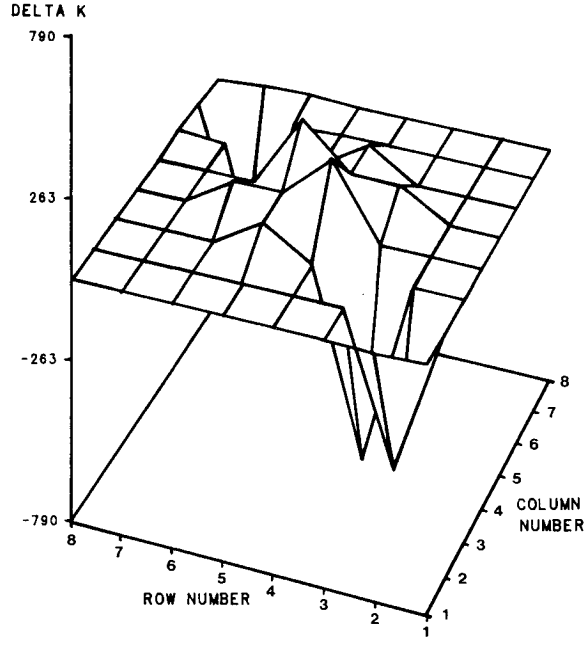

Fig. 5 Graphical presentation of LQO results with corrupted modes.

Table 7 Comparison between TSHAPE NASTRAN and measured modes

Mode no.	Measured frequency, Hz	NASTRAN computed frequency, Hz	Discrepancy, %	Mode description	
				Horizontal plate	Vertical plate
1	13.04	12.23	6.2	No motion	First bending
2	19.76	19.15	3.1	First torsion	Rotation
3	30.56	27.15	11.1	No motion	First torsion
4	32.65	32.37	0.9	First bending	Translation
5	79.54	74.38	6.4	No motion	Bidirectional bending
6	112.80	115.09	2.0	Corners	Second bending
7	114.16	117.18	2.6	Corners	Bidirectional bending
8	119.22	122.57	2.8	Corners	No motion
9	119.77	123.20	2.9	Corners	No motion
10	129.19	130.29	0.9	Second bending	Second bending
11	161.97	155.73	0.1	Second bending	Bidirectional bending
12	176.85	177.11	0.1	Second bending	Bidirectional bending
13	207.95	213.79	2.8	Second bending	Second bending
14	226.24	231.17	2.2	Second bending	Bidirectional bending
15	256.52	254.12	0.9	Bidirectional bending	Bidirectional bending
16	261.17	269.19	3.1	Second bending on edge	No motion
17	264.16	277.96	5.2	Second bending on edge	No motion
18	300.09	307.57	2.5	Bidirectional bending	Bidirectional bending
19	312.62	317.58	1.6	Bidirectional bending	Bidirectional bending
20	331.06	345.73	4.4	Bidirectional bending	No motion

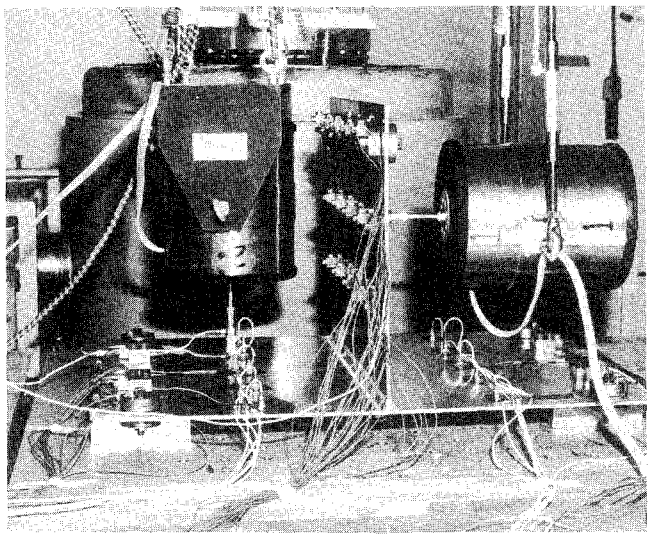

Fig. 6 TSHAPE structure testing.

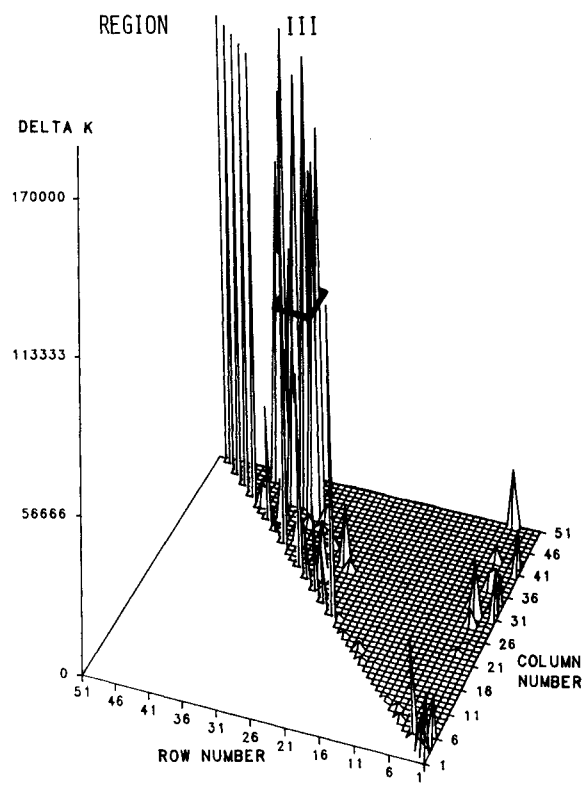

Fig. 7 TSHAPE LQO results with measured modes (decreased stiffness coefficients).

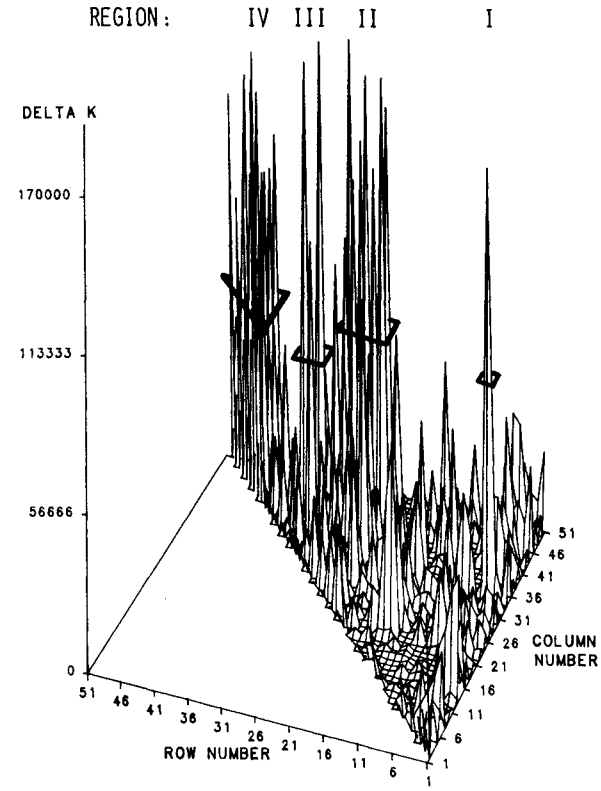

Fig. 8 TSHAPE LQO results with measured modes (increased stiffness coefficients).

Table 6 LQO results with corrupted modes

			LQO results	
			Without corruption	With Φ_1. Φ_2 corrupted
Coefficient	Corrupted stiffness coefficient	Exact stiffness coefficient	4 modes	4 modes
1.1	2.0	1.5	1.5	3.1
1.2	−2.0	−1.5	−1.4	−6.4
2.2	1512.0	1011.5	1011.2	1026.3
2.3	−10.0	−10.0	−10.0	−10.1
3.3	1710.0	1110.0	1110.0	1109.5
3.5	−200.0	−100.0	−100.0	−99.5
4.4	850.0	1100.0	1100.0	1097.7
4.5	−200.0	−100.0	−100.0	−99.6
4.6	−200.0	−100.0	−100.0	−98.6
5.5	850.0	1100.0	1100.0	1100.3
6.6	1714.0	1112.0	1111.9	1100.7
6.7	−10.0	−10.0	−10.1	−17.5
6.8	−4.0	−2.0	−1.9	5.2
7.7	1512.0	1011.5	1011.4	1006.2
7.8	−2.0	−1.5	−1.4	3.8
8.8	6.0	3.5	3.4	−1.8

Conclusion

The numerical and experimental validation of the LQO tool demonstrates the ability of the LQO algorithm to identify and update the coefficients associated with the inappropriately modeled load paths of a structure. The proper use of the LQO algorithm allows a rapid updating effort in a restricted area of the structure analyzed. Such a capability leads to appreciable time savings and more reliable structural models.

Acknowledgments

This research was supported in part by the Communication Research Centre (CRC) of Canada, Supply and Services Canada, under Contract 36100-6-4158/01-ST. The authors wish to express their appreciation to Frank Vigneron (CRC), Yvan Soucy (CRC), and Tom Steel from the David Florida Laboratory (DFL) whose support during the experimental work was invaluable. We wish to also acknowledge lively and helpful discussions on portions of this material with Jaques Gauvin of Ecole Polytechnique de Montreal.

References

[1]Baruch, M. and Itzhack, Y. B., "Optimal Weighted Orthogonalization of Measured Modes," *AIAA Journal*, Vol. 16, April 1978, pp. 346-351.

[2]Baruch, M., "Optimization Procedure to Correct Stiffness and Flexibility Matrices Using Vibration Tests," *AIAA Journal*, Vol. 16, Nov. 1978, pp. 1208-1210.

[3]Berman, A. and Nagy, E. J., "Improvement of a Large Analytical Model Using Test Data," *AIAA Journal*, Vol. 21, Aug. 1983, pp. 1168-1173.

[4]Berman, A. and Wei, F. S., "Automated Dynamic Analytical Model Improvement," NASA CR. 3452, July 1981.

[5]Caesar, B. et al., "Procedures for Updating Dynamic Mathematical Models," Draft Final Report, ESTEC Contract No. 5597/83/NL/PB(SC).

[6]Caesar, B., "Update and Identification of Dynamic Mathematical Models," *Proceedings of the 4th International Modal Analysis Conference*, Union College, Schenectady, NY, Feb. 1986, pp. 394–401.

[7]Chen, J. C. and Wada, B. K., "Matrix Perturbation for Structural Dynamic Analysis," *AIAA Journal*, Vol. 15, Aug. 1977, pp. 1095–1100.

[8]Kabe, A. M., "Constrained Adjustment of Analytical Stiffness Matrices," *Structual Dynamic Testing and Analysis*, SAE, Warrendale, PA, SAE 851932, Oct. 1985, pp. 1–3.

[9]Kabe, A. M., "Stiffness Matrix Adjustment Using Mode Data," *AIAA Journal*, Vol. 23, Sept. 1985, pp. 1431–1436.

[10]Link, M., "Identification of Physical System Matrices Using Incomplete Test Data," *Proceedings of the 4th International Modal Analysis Conference*, Union College, Schenectady, NY, Feb. 1986, pp. 386–393.

[11]Schaeffer, H. G., *MSC/NASTRAN Primer-Static and Normal Modes Analysis*, Wallace Press, New Hampshire, 1982.